

PREPARED FOR SUBMISSION TO JINST

ECPD LISBON CONFERENCE PROCEEDINGS

MAY 6-9, 2019

LISBON

Near-surface measurements of plasma parameters in the Magnum-PSI

J. van den Berg,¹ H.J. van der Meiden, J.W.M. Vernimmen, I.G.J. Classen

*DIFFER - Dutch Institute for Fundamental Energy Research,
De Zaale 20, 5612 AJ Eindhoven, the Netherlands*

E-mail: j.vandenberg@diffier.nl

ABSTRACT: In the quest to long-term operation of high-power magnetically confined fusion devices, it is crucial to control the particle and heat loads on the wall. In order to predict these loads, understanding of the near-surface plasma behaviour is important. This region is marked by plasma acceleration towards the Debye sheath edge. In plasma conditions with high density and low temperature, the interaction between the incoming plasma and recycled neutrals might become important.

In this paper, we present incoherent Thomson Scattering (TS) measurements in the near-surface region of the Magnum-PSI linear plasma generator. To enable TS measurements close to the plasma target of Magnum-PSI, a stray light suppression up to a factor 10^4 was achieved, while retaining high transmission. By incrementally moving the target along the magnetic field, this adapted system was used down to 1.9 mm from the target. In the last 10 – 15 mm in front of the surface, n_e as well as T_e were observed to decrease significantly. For constant particle flux, the density drop indicates plasma acceleration. Thus, under the assumption of ionization and recombination being absent in this region, the measurements can be interpreted to show the plasma presheath, and its lengthscale: ~ 1 cm.

A lower T_e near the wall leads to lower estimations of particle and energy flux at the sheath edge and to the wall. The temperature reduction indicates an energy loss channel for the electrons. Possible causes, related to interaction with recycled neutrals, are discussed.

KEYWORDS: plasma diagnostics, optics, lasers, spectrometers.

¹Corresponding author.

Contents

| | | |
|----------|---|----------|
| 1 | Introduction | 1 |
| 2 | Near-surface incoherent Thomson scattering | 2 |
| 2.1 | Stray light suppression | 2 |
| 2.2 | Measurements | 3 |
| 3 | Discussion | 5 |
| 3.1 | Acceleration & cooling | 5 |
| 3.2 | Interactions in the near-surface region | 5 |
| 3.3 | Addition of coherent Thomson scattering | 6 |
| 4 | Conclusions | 6 |

1 Introduction

In a magnetically confined fusion device, the transport of plasma particles and energy from core to wall commences through a narrow region, called the Scrape-Off Layer (SOL) [3]. To ensure long-term operation of the device, it is crucial to limit and control the plasma load on the wall, and therefore, to understand the processes and interactions in the SOL.

One of the links in this plasma-wall interaction is the electrostatic sheath. Due to the difference in mass, plasma electrons have a very large mobility compared to ions. Due to Debye shielding of the wall, these electrons form a sheath of negative space charge: the Debye sheath. This sheath attracts ions and - in case of an electrically floating wall - ensures an ambipolar outflow of plasma. At the wall, electrons and ions recombine, yielding a flux of neutrals back into the plasma. Therefore, the region of ion acceleration, called the presheath, can also be a region of high neutral density. The collisions between recycled neutrals and the incoming plasma can affect the fluxes of particles and momentum, and thus the plasma load on the wall.

In this paper, we present incoherent Thomson Scattering (TS) measurements in the near-surface region of Magnum-PSI [1], a linear plasma generator in Eindhoven, the Netherlands. Magnum-PSI can reach plasma conditions similar to those in the divertor region of the ITER tokamak [2] in high performance detached operation. The superconducting magnet creates a steady state magnetic field, up to $2.5 T$. A cascaded arc discharge produces a plasma with high electron density $n_e \sim 10^{19} - 10^{21} m^{-3}$ and low temperature $T_e \sim 0.1 - 7 eV$, while a three-stage pumping system ensures a low neutral background density, $< 1 Pa$, in the target chamber. The device has good diagnostic access, enabling measurement of the plasma parameters near the target. However, in order to perform TS closer than $\sim 5 mm$ from the target, stray light mitigation was required. The TS diagnostic set-up is described in section 2 and the stray light mitigation in section 2.1. In section 2.2, we describe the measurements and their results. These are discussed in section 3. Conclusions are presented in section 4.

2 Near-surface incoherent Thomson scattering

The incoherent Thomson Scattering (TS) diagnostic is frequently used for electron density (n_e) and temperature (T_e) measurements in high-density plasmas [4]. Thomson scattering can be described as the scattering of an electromagnetic wave from fluctuations in electron density. If the Debye length of the plasma is large compared to the scattering wavelength ($\frac{2\pi}{k}$ with k the scattering vector wavenumber), scattering occurs dominantly due to thermal fluctuations in electron density. The scattered light is Doppler-shifted, and its spectrum reflects the velocity distribution function of the electrons. Assuming a Maxwellian velocity distribution, a Gaussian fit provides T_e , and using a Rayleigh scattering calibration at a known gas density, the electron density can be obtained.

The TS system in Magnum-PSI [5] consists of a pulsed Nd-YAG laser (0.6 J, 10 Hz) at the second harmonic (532 nm), a 25 m long laser beamline through the vacuum vessel, high transmission collection optics with a linear array of 59 fibers, and finally a high-resolution spectrometer with a transmission grating (which features a very low stray light contribution). An overview of the system is shown in figure 1. The spectrometer images the fiber array onto an ICCD camera. A maximum of 50 spatial positions in the plasma are mapped to the spectra on this image.

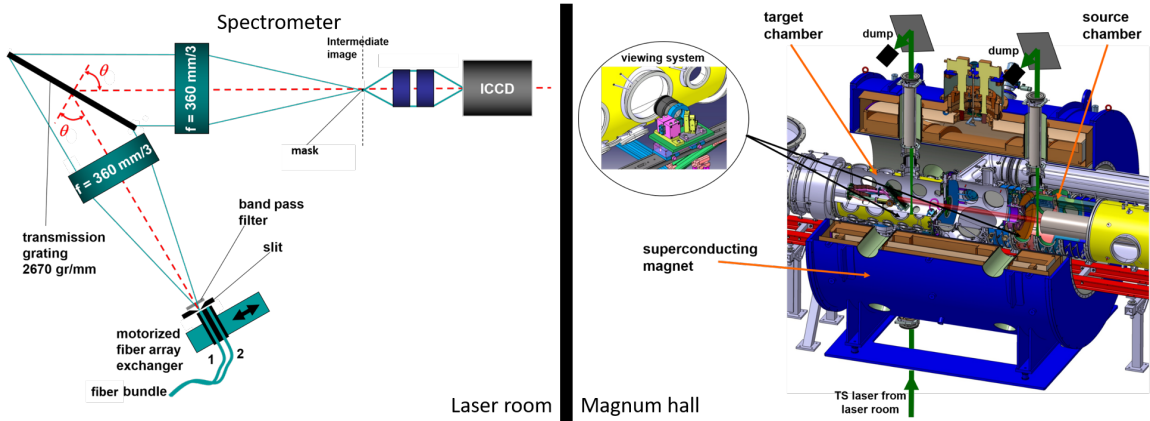


Figure 1. Overview of the TS diagnostic set-up at Magnum-PSI, adapted from [4]. On the right side is a cut-out showing the core of the device, with the plasma beam in red, flowing from source to target mount. The in-vessel beam lines at source and target are shown, with the laser in green. Also depicted is the TS viewing system and fiber connection to the spectrometer in the laser room. An optical drawing of the latter, with intermediate focal plane, is shown on the left side. Bundles 1 & 2 are for the source and target positions, respectively.

2.1 Stray light suppression

The main contribution of stray light is the vacuum window where the TS laser enters the vessel. This light travels upwards, a fraction of it passes the apertures, and - after several reflections in the vessel - a smaller fraction ends up in the viewing system of the diagnostic. On the measured spectrum, the stray light appears as a peak at the laser wavelength, corresponding to the spectrometer instrument function. At the default target-laser distance, $d \approx 30$ mm, the stray light can be

mitigated by subtracting a (vacuum) stray light measurement from the TS spectrum. Moreover, a digital notch is applied in the analysis.

To measure near the surface, the target is moved towards the laser beam. Some stray light from the entrance window will then be reflected directly from the target into the viewing system. This can cause saturation of the ICCD camera. Therefore, physical mitigation was required for this research. The intermediate image of the spectrometer was used, as seen in figure 1. A tandem lens system relays the light to the ICCD camera (as proposed in [5]). A mask of width 0.5 mm was placed in the focal plane, such that it covered the image of the fiber bundle. It is noted here that the width of the mask sets a lower bound on the measurement domain in T_e , in this case at 0.2 eV . To determine the mask's attenuation, two Rayleigh measurements were performed, both in Nitrogen at 50 Pa . The Rayleigh measurements with and without mask are shown in figure 2. The mask resulted in

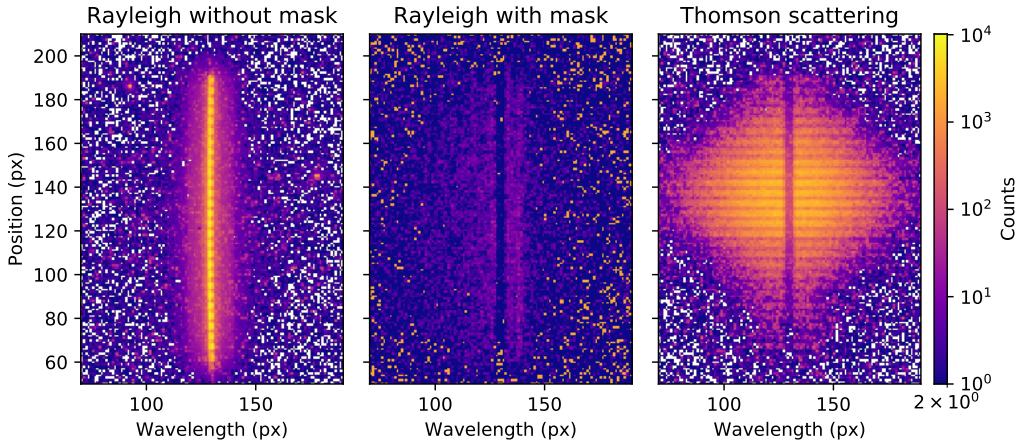


Figure 2. Spectrometer images with the adapted TS set-up, normalized in intensity to 10 laser pulses. From left to right: Rayleigh scattering without mask (30 pulses), Rayleigh scattering with mask (400 pulses), and Thomson scattering (30 pulses) at $B = 1.2\text{ T}$, 7 slm Hydrogen gas flow, $P_n = 1\text{ Pa}$ background pressure and discharge current 175 A , at $d = 32, 2\text{ mm}$. Corresponding background images were subtracted.

a strong reduction of stray light up to a factor 10^4 at the laser wavelength. The measurement with mask shows a feature next to the mask, which is possibly due to internal reflections of stray light in the spectrometer.

The intensity of this feature increased significantly for $d \leq 5\text{ mm}$. Saturation was reached around $d = 1\text{ mm}$.

2.2 Measurements

The adapted set-up enables TS measurements in the vicinity of the target surface. An axial profile of the plasma parameters can be created by incrementally moving the target towards the TS laser. The axial resolution of the measurements is given by the laser beam diameter of $\sim 0.7\text{ mm}$. As can be seen in figure 1, the viewing line of sight is placed in the horizontal plane, perpendicular to the magnetic field. To prevent obstruction of the viewing system ($F/11$ [5]) for small d , a protruding target was used, with diameter 26 mm . This yields a minimal distance $d_{min} = 1.3\text{ mm}$.

For each measurement, 30 laser pulses were accumulated on an image. Five measurements were done per position and setting. Four axial series of measurements were done, from $d = 32 \text{ mm}$ down to the closest possible distance. Stray light images were recorded at each position. The experiments were performed in a Hydrogen discharge with gas flow 7 slm , source current $I = 175 \text{ A}$ and magnetic field 1.2 T . Each series was done with a different (H_2) background pressure: 1, 2, 4 and 8 Pa .

The results of the measurement series at $P_n = 1 \text{ Pa}$ are shown in figure 3. The axial profiles, corresponding to the central positions of the radial profiles (for each P_n) are shown in figure 4.

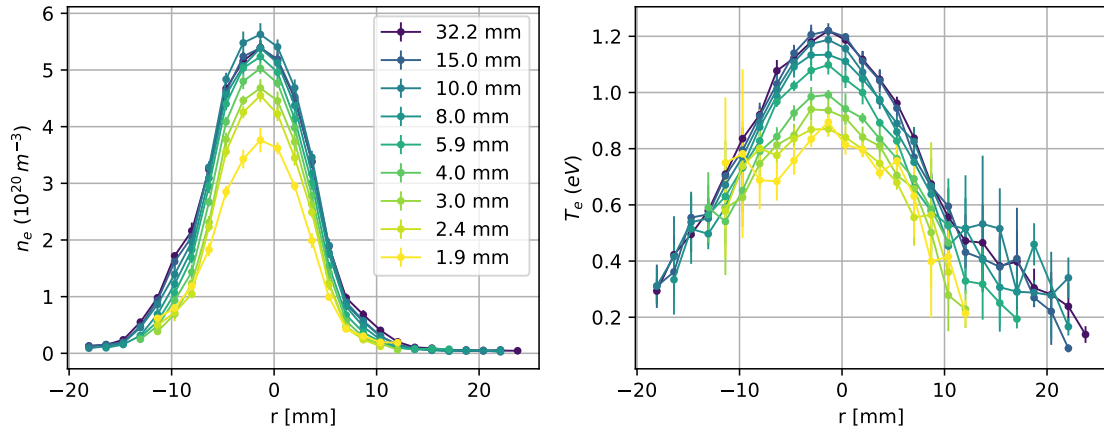


Figure 3. Radial Thomson scattering profiles of electron density (left) and temperature (right), obtained during a steady state Hydrogen discharge in Magnum-PSI, with a magnetic field $B = 1.2 \text{ T}$, discharge current $I = 175 \text{ A}$, gas flow 7.0 slm and with a background pressure of 1 Pa . The errorbars represent the standard deviation over 5 measurements. The profiles are coloured by target distance from the TS position.

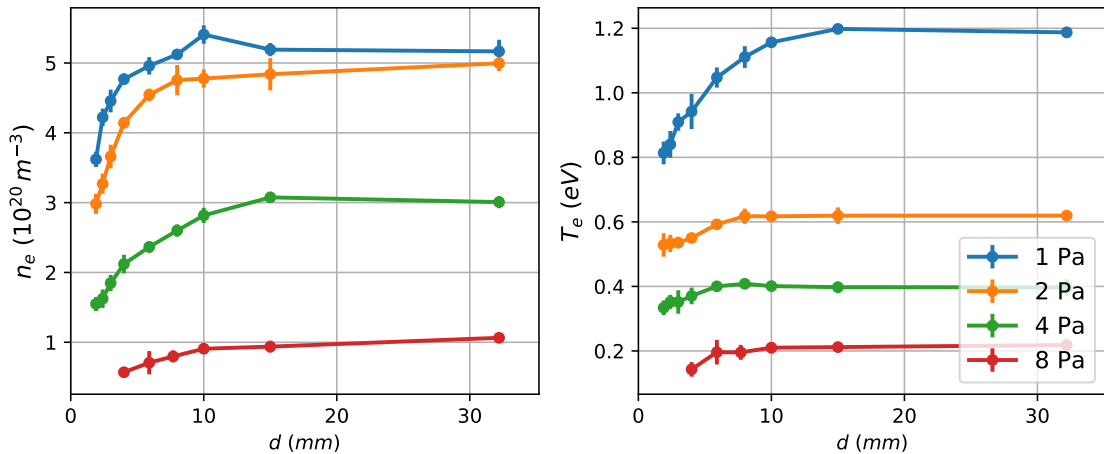


Figure 4. Axial profiles of electron density (left) and temperature (right), as measured by TS in the center of the plasma beam. The profiles are coloured by background pressure.

3 Discussion

Upstream, both n_e and T_e are observed to decrease with the background pressure. As described in [6], this can be attributed to the interaction between plasma and neutrals in the vessel, leading to a loss of static and dynamic pressure (by momentum transfer) and particle flux (recombination).

In all cases, significant decreases of density as well as temperature are observed in the axial direction, amounting to 25 – 50 % for n_e and 15 – 35 % for T_e .

3.1 Acceleration & cooling

The conservation equations of particle and momentum flux in a single-species plasma in 1D are given by:

$$\frac{d}{dx}(nv) = S_{ion} - S_{rec} \quad (3.1a)$$

$$\frac{d}{dx}(m_i n v^2 + n k_B (T_e + T_i)) = S_{mom}, \quad (3.1b)$$

with $n = n_e = n_i$ the plasma density, v the ion drift velocity along the magnetic field, k_B Boltzmann's constant, m_i the ion mass, S_{mom} the momentum source term, and S_{ion} and S_{rec} the particle source terms due to ionization and recombination, respectively. If $S_{ion} - S_{rec} = 0$, the observed axial density drop can only be attributed to plasma acceleration. Thus, if we assume that ionization and recombination are absent, these measurements show us the extent of the plasma presheath: the region of ion acceleration towards the sheath edge. The observed lengthscale of the density drop, ~ 1 cm, coincides with the presheath lengthscale given in [7].

A lower temperature near the surface implies a reduction of the ion sound velocity $c_s = \sqrt{\frac{k_B(T_e + \chi_i T_i)}{m_i}}$ (with χ_i the ion polytropic coefficient) at the sheath edge, resulting in a lower estimation of particle flux to the wall: $\Gamma_{wall} = \Gamma_{se} = n_{se} c_{s,se}$. Moreover, if the electrons have less energy at the sheath edge, the sheath potential difference will be reduced, along with the energy transmission to the wall [3].

3.2 Interactions in the near-surface region

The reduced temperature in the near-surface region implies the presence of an energy sink for the electrons. As stated in section 1, the high density of recycled neutrals near the surface could enhance plasma-neutral interaction. In this section, we discuss several interactions and their possible effect on T_e . Elastic and inelastic electron-neutral collisions can lead to electron cooling directly. Elastic ion-neutral collisions act as a momentum loss term for the plasma (S_{mom} in eq. 3.1b). Through Charge Exchange (CX), ions in the plasma flow are replaced by oppositely moving ions, also causing a significant momentum loss. Due to these sources of drag, the presheath ion acceleration requires a larger electric field. The extra energy necessary to set up this field could be drawn from the electrons.

Finally, volumetric recombination in the near-surface region could also cause electron cooling.

At present, it is unknown whether each of these processes occur, and to what extent. In order to

better understand the near-surface plasma in high-recycling conditions, and to predict the plasma loads on the wall, additional information is needed. Particularly, measurements of ν and T_i would enable solving equations 3.1. Thereby, we could estimate S_{rec} (given S_{ion} is low at $T_e \approx 1 \text{ eV}$) as well as S_{mom} .

3.3 Addition of coherent Thomson scattering

The necessary parameters, ν and T_i , can be measured by employing Coherent Thomson Scattering (CTS). Complementing the incoherent TS that was briefly described in section 2, TS at scattering wavelengths comparable to or larger than the Debye length is said to be in the coherent regime. At these scales, the electron density fluctuations are influenced by plasma waves as well as ion dynamics, i.e. scattering on the electrons is correlated with ion motion, giving ν and T_i .

Recently, a CTS diagnostic was developed for application in low-temperature, high-density plasmas [4]. This diagnostic employs a Nd-YAG laser at 1064 nm that can be superimposed with the TS laser beam, allowing measurements at the same positions. The first measurements with this system have been performed in the former Pilot-PSI device [9]. An upgraded CTS diagnostic is currently being commissioned at Magnum-PSI, and the first measurement report is expected in 2019.

4 Conclusions

In this work, it has been shown that the TS diagnostic at Magnum-PSI can be used down to 1.9 mm from the surface. The necessary stray light mitigation was achieved by placing a mask in the intermediate focus of the TS spectrometer. The resulting measurements show a significant drop in electron density close to the surface. If we assume conservation of particle flux, the presented measurements can be interpreted to show the plasma presheath in Magnum-PSI and its lengthscale: $\sim 1 \text{ cm}$. The measured axial reduction in T_e indicates the presence of an energy sink for the electrons. A lower T_e at the sheath edge leads to lower fluencies of particles and energy to the wall. Possible plasma-neutral interactions that might cause electron cooling include: electron-neutral collisions, ion-neutral collisions and charge exchange.

In future work, the combination of incoherent and coherent TS diagnostics is foreseen, in order to locally solve the conservation equations of particle and momentum flux. Thus, we can expand our knowledge on interaction processes in the near-surface region under ITER-relevant plasma conditions.

References

- [1] G. De Temmerman et al. *High heat flux capabilities of the Magnum-PSI linear plasma device*, Fusion Engineering and Design **88 (6-8)** (2013) pg 483- 487. <https://doi.org/10.1016/j.fusengdes.2013.05.047>
- [2] R.A. Pitts et al. *Physics basis and design of the ITER plasma-facing components*, Journal of Nuclear Materials **415 (1)** (2011) pg S95- S964. <https://doi.org/10.1016/j.jnucmat.2011.01.114>.

- [3] P.C. Stangeby, *The Plasma Boundary of Magnetic Fusion Devices*, IOP Publishing, ISBN 0750305592 (2001) <https://doi.org/10.1088/0741-3335/43/2/702>
- [4] H.J. van der Meiden et al., *Thomson scattering on low and high temperature plasmas*, PhD thesis, ISBN 9789038624556 (2011)
- [5] H.J. van der Meiden et al., *Advanced Thomson scattering system for high-flux linear plasma generator*, *Review of Scientific Instruments* **83** 123505 (2012).
- [6] K.Ješko et al., *Plasma pressure and particle loss studies in the Pilot-PSI high flux linear plasma generator*, *Nuclear Materials and Energy* **12** (2017) pg 1088- 1093.
<https://doi.org/10.1016/j.nme.2017.03.025>
- [7] A. E. Shumack, *The influence of electric fields and neutral particles on the plasma sheath at ITER divertor conditions*, PhD thesis, ISBN 9789038625126 (2011) <https://doi.org/10.6100/IR712706>
- [8] S. Kuhn et al., *Link between fluid and kinetic parameters near the plasma boundary*, *Physics of Plasmas* **13** (1) (2006) pg 1- 8. <https://doi.org/10.1063/1.2161181>
- [9] H.J. van der Meiden et al. *Collective Thomson scattering system for determination of ion properties in a high flux plasma beam*, *Applied Physics Letters* **109** (26) 261102 (2016).
<https://doi.org/10.1063/1.4973211>